

## Journal Pre-proofs

Development of fast-dissolving dosage forms of curcuminoids by electrospinning for potential tumor therapy application

Krisztina Kiss, Kristóf Hegedüs, Panna Vass, Diána Vári-Mező, Attila Farkas, Zsombor Kristóf Nagy, László Molnár, József Tóvári, Gábor Mező, György Marosi

PII: S0378-5173(21)01133-9  
DOI: <https://doi.org/10.1016/j.ijpharm.2021.121327>  
Reference: IJP 121327

To appear in: *International Journal of Pharmaceutics*

Received Date: 16 July 2021  
Revised Date: 24 November 2021  
Accepted Date: 25 November 2021

Please cite this article as: K. Kiss, K. Hegedüs, P. Vass, D. Vári-Mező, A. Farkas, Z. Kristóf Nagy, L. Molnár, J. Tóvári, G. Mező, G. Marosi, Development of fast-dissolving dosage forms of curcuminoids by electrospinning for potential tumor therapy application, *International Journal of Pharmaceutics* (2021), doi: <https://doi.org/10.1016/j.ijpharm.2021.121327>

This is a PDF file of an article that has undergone enhancements after acceptance, such as the addition of a cover page and metadata, and formatting for readability, but it is not yet the definitive version of record. This version will undergo additional copyediting, typesetting and review before it is published in its final form, but we are providing this version to give early visibility of the article. Please note that, during the production process, errors may be discovered which could affect the content, and all legal disclaimers that apply to the journal pertain.

© 2021 Published by Elsevier B.V.



## Development of fast-dissolving dosage forms of curcuminoids by electrospinning for potential tumor therapy application

**Krisztina Kiss<sup>a,b,c</sup>, Kristóf Hegedüs<sup>d</sup>, Panna Vass<sup>a,\*</sup>, Diána Vári-Mező<sup>e</sup>, Attila Farkas<sup>a</sup>, Zsombor Kristóf Nagy<sup>a</sup>, László Molnár<sup>c</sup>, József Tóvári<sup>e</sup>, Gábor Mező<sup>b,f</sup>, György Marosi<sup>a</sup>**

<sup>a</sup> Department of Organic Chemistry and Technology, Budapest University of Technology and Economics (BME), H-1111 Budapest, Hungary

<sup>b</sup> ELKH-ELTE Research Group of Peptide Chemistry, Eötvös Loránd University, H-1117 Budapest, Hungary

<sup>c</sup> Tavanta Therapeutics Hungary Zrt., H-1138 Budapest, Hungary

<sup>d</sup> Institute of Organic Chemistry, Research Centre for Natural Sciences, H-1111 Budapest, Hungary

<sup>e</sup> National Institute of Oncology, Department of Experimental Pharmacology, H-1122 Budapest, Hungary

<sup>f</sup> Institute of Chemistry, Eötvös Loránd University, H-1117 Budapest, Hungary

\* Corresponding author, H-1111 Budapest, Múgyetem rakpart 3, Hungary;  
panna.vass@oct.bme.hu

## Abstract

Curcuminoids (CUs) of antitumor and various other potential biological activities have extremely low water solubility therefore special formulation was elaborated. New fast dissolving reconstitution dosage forms of four CUs were prepared as fibrous form of 2-hydroxypropyl- $\beta$ -cyclodextrin (HP- $\beta$ -CD). In the electrospinning process HP- $\beta$ -CD could act both as solubilizer and fiber-forming agent. The solubilization efficiency of the CU-HP- $\beta$ -CD systems was determined with phase-solubility measurements. The electrospun CUs were amorphous and uniformly distributed in the fibers according to XRD analysis and Raman mappings. The fibrous final products had fast (<5 min) and complete dissolution. In typical iv. infusion reconstitution volume (20 mL) fibers containing 40-80 mg of CU could be dissolved, which is similar to the currently proposed dose (<120 mg/m<sup>2</sup>). The *in vitro* cytostatic effect data showed that the antitumor activity of the CU-HP- $\beta$ -CD complexes was similar or better compared to the free APIs.

## Keywords

Curcuminoids, Curcumin, Cyclodextrin, Aqueous electrospinning, Fast-dissolving

## Abbreviations

API, active pharmaceutical ingredient; CCD, charge-coupled device; CD, cyclodextrin; CLS, classical least squares; CU, Curcuminoid; CUR, Curcumin; DSC, Differential scanning calorimetry; ES, electrospinning; HP- $\beta$ -CD, 2-hydroxypropyl- $\beta$ -cyclodextrin; HSES, high-speed electrospinning; iv., intravenous; PEG, polyethylene glycol; PM, physical mixture; SEM, scanning electron microscopy; TG, thermogravimetric; XRD, X-ray diffraction;  $\beta$ -CD,  $\beta$ -cyclodextrin;

## 1. Introduction

Curcuminoids (CUs) are the main components of turmeric a spice constituent derived from the plant *Curcuma longa*. The major curcuminoids present in turmeric are curcumin (**Fig. 1.a**), demethoxycurcumin (**Fig. 1.b**), *bis*-demethoxycurcumin (**Fig. 1.c**) and cyclocurcumin (**Fig. 1.d**).

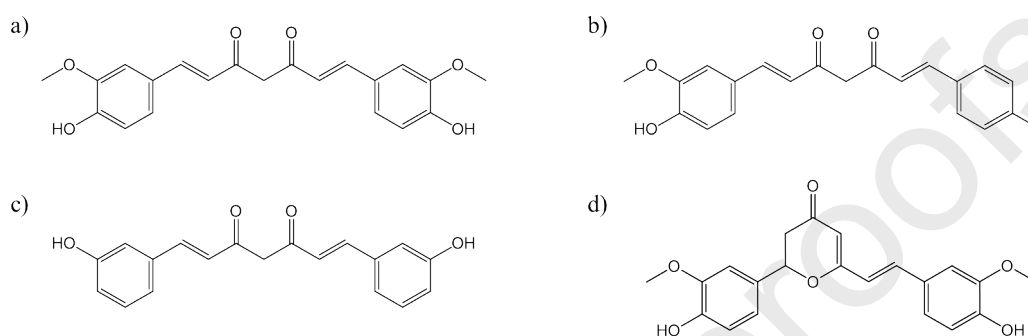


**Figure 1.** The main components of tumeric; a) curcumin (CUR), b) demethoxycurcumin, c) *bis*-demethoxycurcumin, d) cyclocurcumin.

Curcuminoids belong chemically to the group of linear diaryl heptanoids. Their seven-membered carbon chain contains an oxy-substituted aryl moiety at both ends and a 1,3-keto-enol moiety. The C7 chain is generally unsubstituted, except for the 1,3-diketone groups. The 1,3-diketone group exhibits keto-enol tautomerism, the *bis*-keto form dominates in acidic and neutral conditions, whereas the enolic form dominates under alkaline conditions. The aryl moieties could be symmetrically or asymmetrically substituted. (**Fig. 2**)

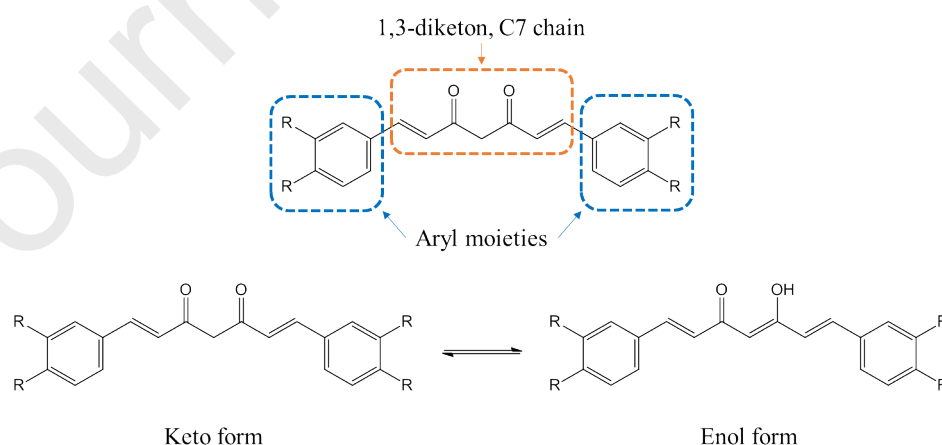


**Figure 2.** General structure of curcuminoids and their keto-enol tautomerism.

Research over the last few decades has shown that curcuminoids have a wide range of biological activities. There are a few examples are antioxidant (Amalraj et al., 2017; Menon and Sudheer, 2007; Sökmen and Akram Khan, 2016), anti-inflammatory (Amalraj et al., 2017; Bagad et al., 2013; Menon and Sudheer, 2007), cardioprotective (Amalraj et al., 2017), *etc.*, and also anticancer (Amalraj et al., 2017; Gupta et al., 2017; Reddy et al., 2013; Tomeh et al., 2019) applications. Curcumin is being extensively researched as a potent antitumor API, the studies showed that it induces apoptotic cell death and inhibits proliferation of cancer cells through regulation of various factors and enzymatic routes (Giordano and Tommonaro, 2019; Kuttikrishnan et al., 2019; Li et al., 2017; Mansouri et al., 2020; Shehzad et al., 2013). It affects a wide range of tumor cells (breast (Wang et al., 2016), bone (Chen et al., 2017), pulmonary (Amalraj et al., 2017), digestive system (Bahrami and A. Ferns, 2020), *etc.* cancers), due to the broad mechanism of action in terms of antitumor activity.

However, curcuminoids have low bioavailability, which hinders their therapeutic efficiency. Oral administration results in extremely low serum levels (Yang et al., 2007). To increase the bioavailability addition of adjuvants, the formation of liposomes and phytosomes are currently used (Kurita and Makino, 2013). Curcumin is well tolerated even in high doses (8-12 g/day) orally (Lao et al., 2006), however, studies showed that in prolonged use (1-4 months) even lower doses (0.9-3.6 g/day) could induce some adverse effects (nausea and diarrhea) and could cause even chest tightness, inflamed skin, and skin rashes (Lao et al., 2006; Sharma et al., 2004).

The intravenous (iv.) administration route could solve the low absorption and bioavailability by bypassing the GI tract and could also solve the adverse effects experienced during prolonged use by oral administration (Chien, 1991). Moreover, a suitable iv. administration form could be easily incorporated into current chemotherapy treatments. However, due to the extremely low water solubility, an appropriate innovative formulation is needed. Mainly, there are two approaches to produce CUR containing iv. products. One approach is emulsion based: e.g. ImprimisRx's Compounded Curcumin Emulsion Product for Injection, however, a mayor downfall of this method is that the applied PEG (polyethylene glycol) 40 castor oil excipient caused hypersensitivity reactions and even death in patients, therefore the FDA investigated this product (FDA, 2017). The more promising approach is liposomal CUR (Bulboacă et al., 2018; Greil et al., 2018; Storka et al., 2015). However, Storka et al. (Storka et al., 2015) mentioned an adverse effect, namely, the liposomal curcumin induced transient changes in red blood cell morphology, however, it was reversible. Examined from an industry perspective, liposomal iv. products are produced by batch technology with high-energy consumption

(Wagner and Vorauer-Uhl, 2011). Moreover, preparation and characterization of liposomal products is challenging.

With the use of 2-hydroxypropyl- $\beta$ -CD (HP- $\beta$ -CD), processed with electrospinning (ES), the previously mentioned problems could be overcome. HP- $\beta$ -CD is safe, and FDA approved pharmaceutical excipient even in an iv. administration form, due to the low molecular weight and low toxicity (Gould and Scott, 2005; Loftsson et al., 2005). Owing to the high water-solubility and complexation capability of HP- $\beta$ -CD, this innovative formulation approach could solve the solubility shortcomings of CUs. CDs having lipophilic central cavity forms easily an inclusion complex with a lipophilic compound (such as CU) or moiety. The hydrophilic outer surface of the HP- $\beta$ -CD molecule grants that the formed inclusion complex is highly water-soluble (Brewster and Loftsson, 2007).

With electrospinning (ES), drug-loaded nano- or microfibers can be prepared from a viscous polymer or CD solutions. During the ES process, the dried fibers are formed by electrostatic forces. Lately, ES has been a popular method in researches to produce pharmaceutical products, more specifically drug delivery systems for a wide range of applications (Al-Attar and Madhally, 2019; Allafchian et al., 2020; Celebioglu and Uyar, 2021; Razzaq et al., 2021; Sasmal and Datta, 2019; Tuğcu-Demiröz et al., 2020). Like in freeze-drying, the final product is usually an amorphous solid dispersion (Tipduangta et al., 2021), which provides fast dissolution (Balogh et al., 2015; Topuz and Uyar, 2019). Moreover, electrospun fibers have a large surface area that further increases the dissolution rate. Newer, sophisticated types of drug-loaded products made by ES to provide modified dissolution properties are e.g. core-shell (Ding et al., 2020; Zare et al., 2021), Janus fibers (Zheng et al., 2021) or Janus beads (Li et al., 2021). Additionally, ES is a continuous and energy-efficient process that satisfies current industrial aspirations toward continuous manufacturing. Further improving the compatibility to pharma industry a high-speed electrospinning (HSES) device was developed to produce fibrous amorphous solid dispersions even in pilot-scale (Nagy et al., 2015). During this process the electrostatic fiber elongation is supported with high-speed rotational jet generation (Sebe et al., 2013), improving this way the productivity. The crucial part of this device is the rotating spinneret (containing numerous orifices), which minimizes the free liquid surface.

Electrospinning of curcumin-containing fibers is not a new topic in the literature. Several different approaches have been investigated, but the product application options proposed so far have been rather limited. Most studies investigate the antimicrobial or antioxidant effect of

curcuminoids and the possibilities for improving the aqueous solubility of these poorly soluble (Awan et al., 2020; Celebioglu and Uyar, 2021; Kanu et al., 2020; Ramalingam et al., 2015; Shababdoust et al., 2018; Sun et al., 2013; Topuz and Uyar, 2019). Curcumin loaded fibers have been prepared using polyurethane (Shababdoust et al., 2018), poly(2-hydroxyethyl methacrylate) (Ramalingam et al., 2015), polyvinylpyrrolidone and polyvinylpyrrolidone/ $\beta$ -CD (Sun et al., 2013), Eudragit RS 100 (copolymer of ethyl acrylate, methacrylate and methacryl acid ester) (Awan et al., 2020). For sustained release, curcumin have even been loaded into gelatin (Kanu et al., 2020).

HP- $\beta$ -CD as a host molecule in CUR ICs application was suggested by Ouyang (Ouyang et al., 2012). Later it was used in formulation processes as common solvent evaporation and freeze drying (Jantarat et al., 2014). Lately, CUR- HP- $\beta$ -CD complexes were also electrospun, and the prepared fibers were mainly used as potential antioxidant products. Aytac et al. (Aytac and Uyar, 2017) presented electrospun core-shell nanofibers of CUR-HP- $\beta$ -CD complex and PLA (polylactic acid), or fast-dissolving antioxidant CUR-HP- $\beta$ -CD nanofibers without any added polymer (Celebioglu and Uyar, 2020).

However, no research was found in the literature on CUR-HP- $\beta$ -CD or CU-HP- $\beta$ -CD electrospun complexes developed for potential iv. administration. Therefore, the aim of this work was to develop a fast dissolving reconstitution formulation (for potential iv. application) of several CU-HP- $\beta$ -CD complexes prepared by ES. Moreover, to show that the developed formulation process could be scaled-up without any further optimization of the electrospinning solution was also planned. Lastly the general goal was the evaluation of the potential applicability of electrospun CU- HP- $\beta$ -CD complexes in tumor therapy.

## 2. Materials and methods

### 2.1. Materials

Curcumin (**Fig. 3.a**) was purchased from VWR International Kft. (Debrecen, Hungary). The curcumin analogues ((1E,6E)-1,7-*bis*(3-hydroxy-4-methoxyphenyl)hepta-1,6-diene-3,5-dione, (1E,6E)-1,7-*bis*(3-hydroxyphenyl)hepta-1,6-diene-3,5-dione and *bis*-demethoxycurcumin) (**Fig. 3.b-d**) were synthesized by the authors (**Supp. Info.**). HP- $\beta$ -CD (**Fig. 3.e**) (Kleptose<sup>®</sup> HPB, average degree of substitution = 0.62) was obtained from Roquette (Lestrem, France). The water used was from a Millipore Milli-Q<sup>®</sup> ultrapure water system (Millipore, Billerica, MA, USA).

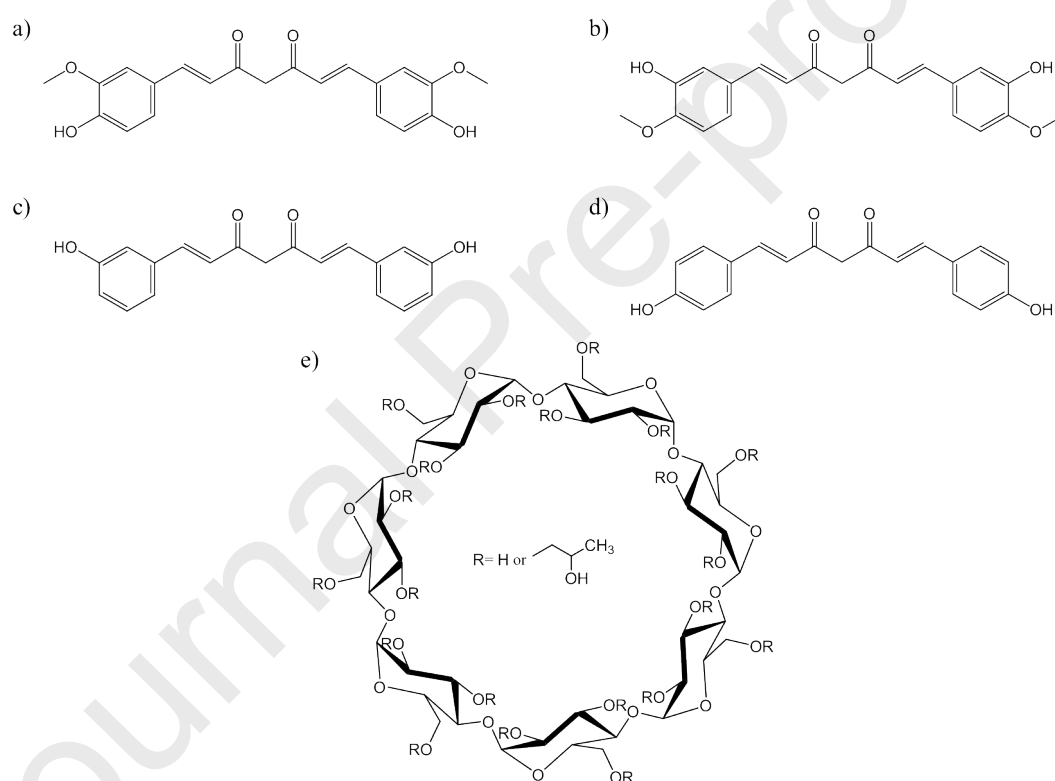


**Figure 3.** The structure of a) curcumin (CUR), b) (1E,6E)-1,7-*bis*(3-hydroxy-4-methoxyphenyl)hepta-1,6-diene-3,5-dione (CU2), c) (1E,6E)-1,7-*bis*(3-hydroxyphenyl)hepta-1,6-diene-3,5-dione (CU3), d) *bis*-demethoxycurcumin (CU4), and e) 2-hydroxypropyl- $\beta$ -cyclodextrin (HP- $\beta$ -CD).

## 2.2. Lab-scale high-speed electrospinning

The electrospinning experiments were performed with a lab-scale high-speed electrospinning (HSES) system. The spinneret was connected to a high-speed motor coupled with a high voltage supply (MA2000, Nagykanizsa, Hungary). The used spinneret diameter was 34 mm and contained 8 orifices with a diameter of 330  $\mu\text{m}$ . A SEP-10S Plus type syringe pump (Aitecs, Vilnius, Lithuania) dosed the CU-HP- $\beta$ -CD complex solutions (**Fig. 4**). The high-speed motor was set to 10,000 rpm and the applied electrical potential to the spinneret was 35 kV, while the feeding rate was 30 mL/h. The sample collection time was 20 minutes. The grounded metal collector was covered with aluminum foil and the distance was 40 cm from the spinneret. The used viscous solution content is indicated for each CU in **Table 1**, the components were added to purified water and stirred (600 rpm) at room temperature – covered with aluminum foil – until complete dissolution. The experiments were performed at ambient conditions.

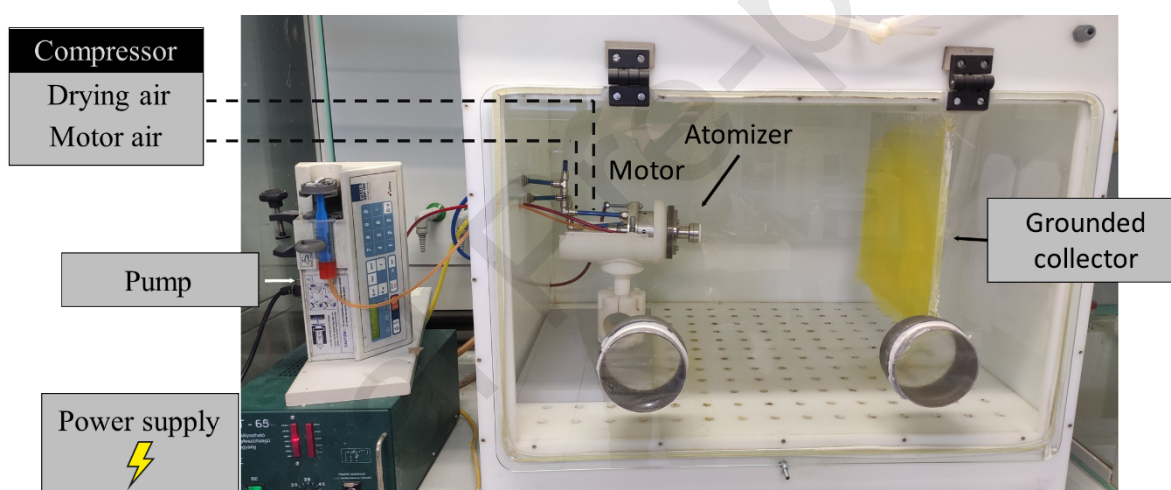


**Figure 4.** Lab-scale HSES device with a grounded plate collector.

### 2.3. Pilot-scale high-speed electrospinning

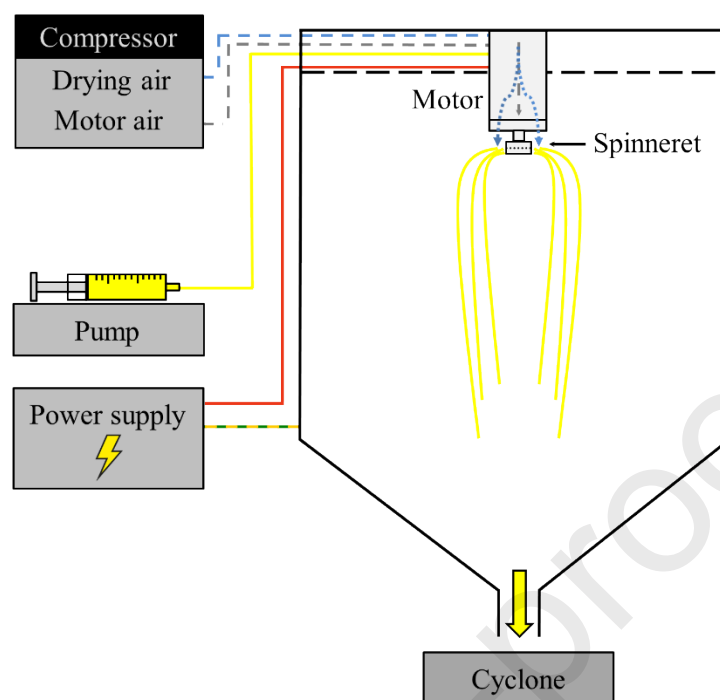


**Figure 5.** High-speed electrospinning (HSES) device with a cyclone collector.

The scaled-up production was carried out with a pilot-scale HSES system (due to the limited availability of the curcuminoids, only the commercially bought CUR was processed with pilot-scale HSES). The pilot-scale device is comparable to the previously presented lab-scale system; therefore, the stainless-steel spinneret is connected to a high-speed motor (**Fig. 5**). The spinneret contained 36 orifices ( $d=330\ \mu\text{m}$ ) in a diameter of 34 mm. For the pilot-scale experiment CUR (0.48 w/w%) and HP- $\beta$ -CD (68.00 w/w%) were added to purified water (31.52 w/w%). The mixture was covered with aluminum foil and stirred at 600 rpm until complete dissolution with a magnetic stirrer. The electrospinning solution was fed with a SEP-10 S Plus syringe pump (Aitecs, Vilnius, Lithuania) with a flow rate of 120 mL/h. The applied voltage was 40 kV (power supply: Unitronik Ltd., Nagykanizsa, Hungary) and the spinneret's rotational speed was fixed at 40,000 rpm. A cyclone was responsible for collecting the produced fibrous material and the collection time was 40 minutes. The experiment was performed at ambient conditions.

### 2.4. Grinding of the electrospun material

The electrospun materials were pushed through a sieve with a 1.0 mm hole size to improve the manageability and flowability of the fibers.

## 2.5. Scanning electron microscopy (SEM)

Morphology of the fibrous CUs was investigated by a JEOL 6380LVa (JEOL, Tokyo, Japan) type scanning electron microscope. The samples were fixed with conductive double-sided carbon adhesive tape, then – to avoid electrostatic charging – the specimens were sputter-coated with gold prior to the examination. The applied accelerating voltage and working distance were set to 8 kV and 20 mm, respectively. The diameters of the fibers were measured directly on the SEM image with the built-in evaluation tool of the JEOL SEM analysis software (supplied with the equipment; approx. 20 fibers were measured in each sample).

## 2.6. X-ray diffraction (XRD)

X-ray diffraction (XRD) patterns were recorded by a PANanalytical X'pert Pro MDP X-ray diffractometer (Almelo, The Netherlands) using Cu-K $\alpha$  radiation (1.542 Å) and Ni filter. The applied voltage was 40 kV while the current was 30 mA. The electrospun samples (**Table 1.**) and the references were analyzed for angles  $2\theta$  between 4° and 42°. The physical mixtures had the same CU content as specified in **Table 1.**, the powders were manually mixed thoroughly after weighing.

## 2.7. Thermogravimetric analysis (TG)

The residual water content of the samples was measured with a TGA55 instrument (TA Instruments, New Castle, DE, USA). The samples were heated linearly from 25 to 105 °C with 10 °C/min, then it was kept at 105 °C for 10 min. A nitrogen atmosphere was used during the measurement, the applied nitrogen flush was 50 mL/min.

## 2.8. Differential scanning calorimetry (DSC)

The electrospun samples and their references were measured with a DSC2500 instrument (TA Instruments, New Castle, DE, USA). The heating rate was 10 °C/min, the samples (sample weight: 3-5 mg; aluminum Tzero™ pan with lid) were heated from 25 to 250 °C. The measurements were performed with nitrogen flush (50 mL/min).

## 2.9. Raman mapping

The homogeneity of selected fibrous samples was evaluated with a Labram-type Raman instrument of Horiba Jobin–Yvon (Kyoto, Japan) coupled with an Olympus BX-40 optical

microscope and an external 785 nm diode laser source. In the high-resolution measurements an objective of 100× (laser spot size: ~2 μm) was used. A 950 groove/mm grating monochromator dispersed and directed the Raman photons to the CCD detector. The measurements were carried out with 5 cm<sup>-1</sup> spectral resolution on the spectral range of 459–1676 cm<sup>-1</sup>. The maps were collected with a 2 μm step size in both directions and consisted of 31×31 points. One spectrum acquisition took 30 s and accumulated 2 times in each mapping point. The evaluation was carried out by the classical least squares (CLS) method using the spectra of the reference substances. The amorphous API references were extracted from the spectra of the fibrous materials.

### 2.10. Dissolution test

The same spectrophotometer and general method were used during the UV-VIS measurements of the dissolution solutions as described in **Supporting Info** (Section 2).

A dissolution test of the electrospun sample was carried out in a small amount of water (1.5 mL). 800 mg ground electrospun samples – containing CUs defined in **Table 1** – were weighed into a glass vial. 1.5 mL purified water was added into the vials, which were then shaken vigorously for 5 min, then the UV-VIS measurements were carried out.

In order to evaluate the improved solubility of the new formulation two selected electrospun sample was further tested. In this test, the electrospun samples and the physical mixtures were compared. The test was also carried out in 1.5 mL water but the dissolution process was followed with pictures using a digital camera and with UV-VIS measurements at predetermined time (30 s, 2 min, and 5 min) intervals.

Moreover, a higher amount (carried out in 20 mL water) of an electrospun sample (6 g; containing 42.0 mg of CUR) was also evaluated with the previous process.

In all cases before the concentration measurements, the solutions were filtered through regenerated cellulose filters with 0.45 μm pores. The filtered solutions were diluted as needed. One sample point is compiled from 3 separate UV-VIS measurements of the same solution. The results were corrected with the water content of the samples.

### 2.11. Cell culturing and *in vitro* cytostatic effect studies

In experimental procedures following cell lines were used, MDA-MB-231 (human breast cancer), A2058 (human melanoma), HT-29 (human colorectal adenocarcinoma) were cultured in RPMI 1640 Medium with glutamine (Biosera, Nuaille, France) and PANC-1 (human pancreatic cancer) were cultured in Dulbecco's Modified Eagle's Medium (Lonza, Verviers, Belgium). All media were supplemented with 10 v/v% heat-inactivated FBS (Fetal Bovine Serum; Biosera, Nuaille, France) and 1 v/v% penicillin/streptomycin (Lonza, Verviers Belgium). The cell lines were mainly obtained from ATCC, except for A2058 (kindly provided by L.A. Liotta, NCI, Bethesda, MD, USA). Cells were cultured in sterile T25 or T75 flasks with ventilation cap (Sarstedt, Nümbrecht, Germany) at 37 °C in a humidified atmosphere with 5% CO<sub>2</sub>.

To evaluate the *in vitro* cytostatic effect of the CU derivatives, MTT assay (3-(4,5-dimethylthiazol-2-yl)-2,5-diphenyl-tetrazolium bromide) (Merck KGaA, Darmstadt, Germany) was carried out. The MTT assay is used to determine IC<sub>50</sub> by measuring cellular metabolic activity as an indicator of cell viability. IC<sub>50</sub> is the concentration of an inhibitor where the tumor cells viability is reduced by half. After harvesting of the cells by trypsin-EDTA (Lonza, Verviers Belgium),  $4 \times 10^3$  till  $7 \times 10^3$  cells per well (depending on cell line), were seeded in complete growth medium consisting of respective basic medium, 10 v/v% heat-inactivated FBS, and 1 v/v% penicillin/streptomycin to 96-well plates (Sarstedt, Nümbrecht, Germany) and incubated. After 24 h, cells were treated with various concentrations (9-series dilution, dilution factor = 3) of CU derivatives starting from 100 µM concentration in growth medium. The control wells were treated with only growth medium. After 72 h of treatment, in order to determine cell viability MTT assay was performed by adding 22 µL of MTT solution (5 mg/mL in PBS) to each well and after 3 h of incubation at 37 °C, the supernatant was removed. The formazan crystals were dissolved in a 50-50 v/v% solution of DMSO (Merck KGaA, Darmstadt, Germany) and EtOH (Molar Chemicals Kft., Halásztelek, Hungary) and the absorbance was measured after 15 min at  $\lambda = 570$  nm by using a microplate reader (BMG Labtech, CLARIOstar Plus, Ortenberg, Germany). The IC<sub>50</sub> values of the CU derivatives were calculated using GraphPad Prism 6 (GraphPad Software, San Diego, CA, USA). The experiments were done in triplicates and each experiment was repeated twice.

### 3. Results and discussion

#### 3.1. Determination of the composition of electrospinning solutions

To determine the maximum CU content in the electrospinning solutions, the fitted lines shown in **Fig. S8-S11** (Phase-solubility profile of the CUs; **Supporting Info Section 2**), were converted to CU w/w% as a function of HP- $\beta$ -CD concentration. The starting plateau of the plotted lines in **Fig. 6** (and in **Fig. S12-14, Table 1**) shows the theoretically achievable maximum concentration. To calculate the HP- $\beta$ -CD concentration in the planned reconstitution solution, the API content was neglected (due to the CUs theoretical maximum w/w% concentration was always around 1%). Therefore, 800 mg of final product is equal to 800 mg of HP- $\beta$ -CD in 1.5 mL water, thus the final HP- $\beta$ -CD concentration was 533 mg/mL. In order, to compensate for the lower effectiveness of HP- $\beta$ -CD as a host at higher concentrations, a slightly lower final concentration was selected at 500 mg/mL to determine the CU contents in the electrospinning solutions.

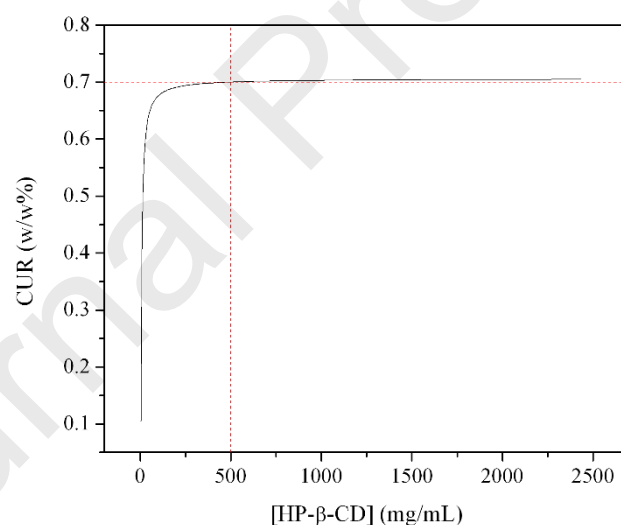


**Figure 6.** Determination of the maximum curcumin (CUR) concentration in the electrospinning solution.

**Table 1.** Composition of the electrospinning solutions and the produced solid materials.

Compound	Concentration (w/w%) in the electrospinning solution	Concentration (w/w%) in the fibers
<b>CUR</b>	0.48	0.70
<b>CU2</b>	0.94	1.38
<b>CU3</b>	0.80	1.17
<b>CU4</b>	0.69	1.02
<b>HPBCD</b>	68.00	varied

The concentration of the fiber-forming agent is considered to be the most critical technological parameter of ES (Nagy et al., 2012), therefore the concentration of HP- $\beta$ -CD in the electrospinning solution was fixed to 68.0 w/w%. Using the maximum CU w/w% ( $CU_{max}$  w/w%) shown in **Table 1** the electrospinning solutions CU content (CU w/w%) could be calculated as follows:

$$CU \frac{w}{w} \% = HP - \beta - CD \frac{w}{w} \% \cdot CU_{max} \frac{w}{w} \% \cdot 10^{-2} = 68.0 \cdot CU_{max} \frac{w}{w} \% \cdot 10^{-2}$$

The summary of the used electrospinning solutions content is shown in **Table 1**.

### 3.2. Formation of CU-HP- $\beta$ -CD fibers with electrospinning (HSES)

The lab-scale HSES experiments were carried out (as discussed in **Materials and methods 2.2.**) using the previously determined aqueous CU-HP- $\beta$ -CD solutions (**Table 1**). The yield was ~75% and the productivity of this system was ~15 g/h in all four cases. Electron microscopic images in **Fig. 7.a-d** show the electrospun CU-HP- $\beta$ -CD fibers. Without exception all four CU-HP- $\beta$ -CD fibers were of good quality, without any fiber defects (e.g.: bead formation, unspun droplets, ribbon-like effects). The diameter range of the fibers was approx. 4-25  $\mu$ m.

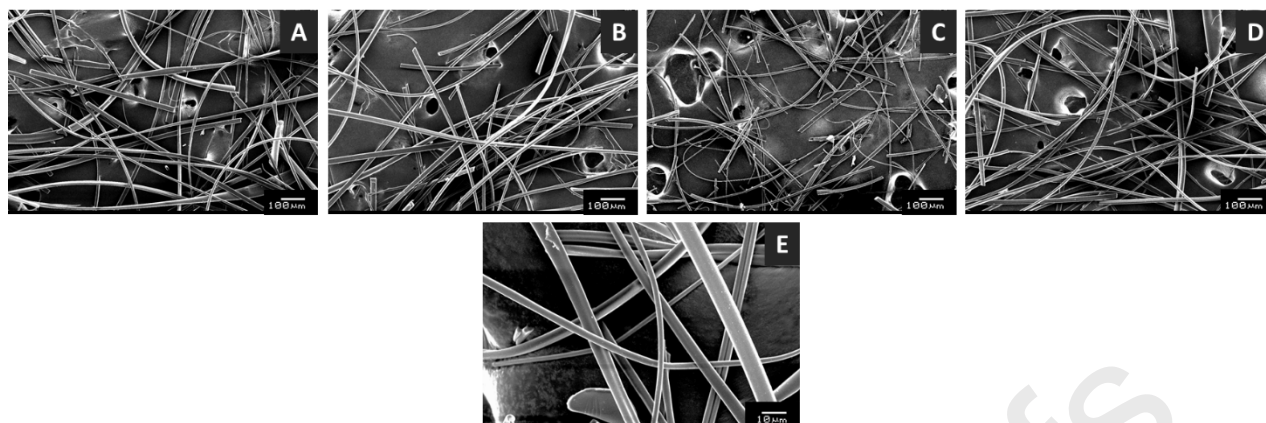


**Figure 7.** Scanning electron microscopic images of the HP- $\beta$ -CD complexes produced by lab-scale HSES (A: curcumin (**CUR**), B: (1E,6E)-1,7-bis(3-hydroxy-4-methoxyphenyl)hepta-1,6-diene-3,5-dione (**CU2**), C: (1E,6E)-1,7-bis(3-hydroxyphenyl)hepta-1,6-diene-3,5-dione (**CU3**), D: bis-demethoxycurcumin (**CU4**) and by pilot-scale HSES (E: curcumin (**CUR**))

Evaluating the scalability higher productivity was tried to achieve from the same solution of CUR-HP- $\beta$ -CD using HSES equipment (**Materials and methods 2.3.**). In this case, the yield was higher (85%). The 10% increase in yield was due to the different orientation of the spinneret (in the pilot-scale HSES system the spinneret was vertical), which increases the formation of fibers. Moreover, the cyclone collector was much more effective to collect the final material, than the commonly used grounded plate. The productivity of the pilot-scale HSES system ( $\sim 80$  g/h) was five times higher than the lab-scale HSES ( $\sim 15$  g/h). According to **Fig. 7.e**, the diameter of the fibers was 3-8  $\mu\text{m}$ , which is less than fibers produced by the lab-scale HSES (4-25  $\mu\text{m}$ ). The difference in the diameters could be explained by the higher (quadruple) spinneret speed applied during the pilot-scale HSES process, which further enhances the elongation during the fiber formation phase.

### 3.3. X-ray diffraction (XRD)

To ensure the fast dissolution during the reconstitution – ideally – the CUs should be in an amorphous physical state in the final fibrous material. In order to investigate the physical state of CUs the final product was compared to the pure crystalline CU and the physical mixture of CU and HP- $\beta$ -CD (which had the same composition as the fibrous product). The characterizations were carried out with X-ray diffraction. The diffractogram of the fibrous product (**Fig. 8, Fig. S15-17**) did not show any of the crystalline CU characteristic peaks, nor

in the physical mixture diffractograms. This indicates that the XRD was not sensitive enough to detect a small volume of crystallites (Balogh et al., 2015). Therefore, another analysis method was needed to determine the CU physical state.

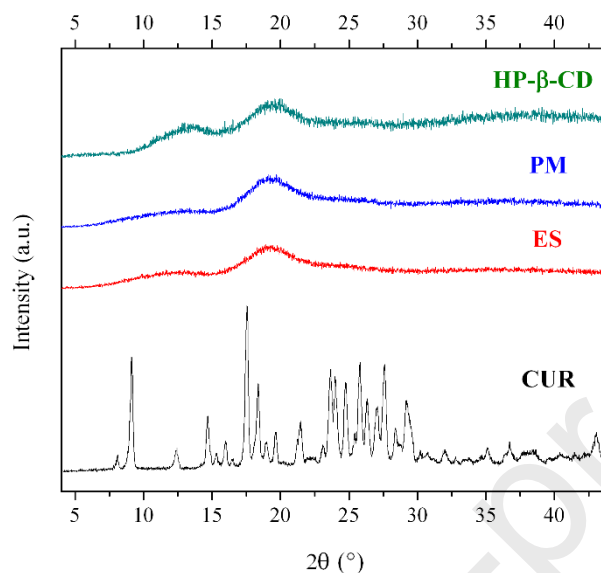


**Figure 8.** X-ray powder diffraction (XRD) patterns of the HP- $\beta$ -CD, the physical mixture of CUR and HP- $\beta$ -CD (PM), the electrospun CUR-HP- $\beta$ -CD complex (ES), and the crystalline CUR.

### 3.4. Differential scanning calorimetry (DSC)

The DSC thermograms (Fig. 9 and in Fig. S18-20) show no endothermic melting peak of CU in the fibrous products, while it can be observed in the physical mixture. Thus, it confirmed that an amorphous solid dispersion was obtained during the ES process (all CUs were amorphous in the fibrous samples).

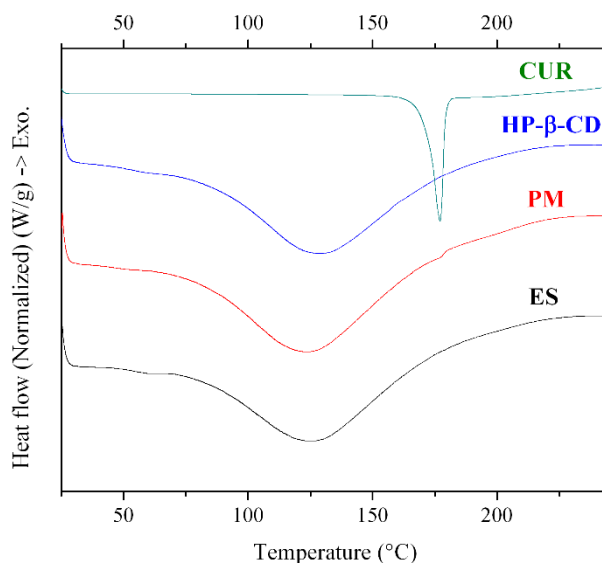


**Figure 9.** Differential scanning calorimetry (DSC) thermograms of the CUR, HP- $\beta$ -CD, the physical mixture of CUR and HP- $\beta$ -CD (PM), the electrospun CUR-HP- $\beta$ -CD complex (ES).

### 3.5. Raman mapping

Out of the 4 electrospun samples containing CUs, two were selected to investigate the distribution of the APIs in the fibers. Raman mapping provides exact information about the local concentration of the API in the fibers. Two fibrous CU-HP- $\beta$ -CDs and their physical mixtures of CU and HP- $\beta$ -CD were compared (**Fig. 10**).

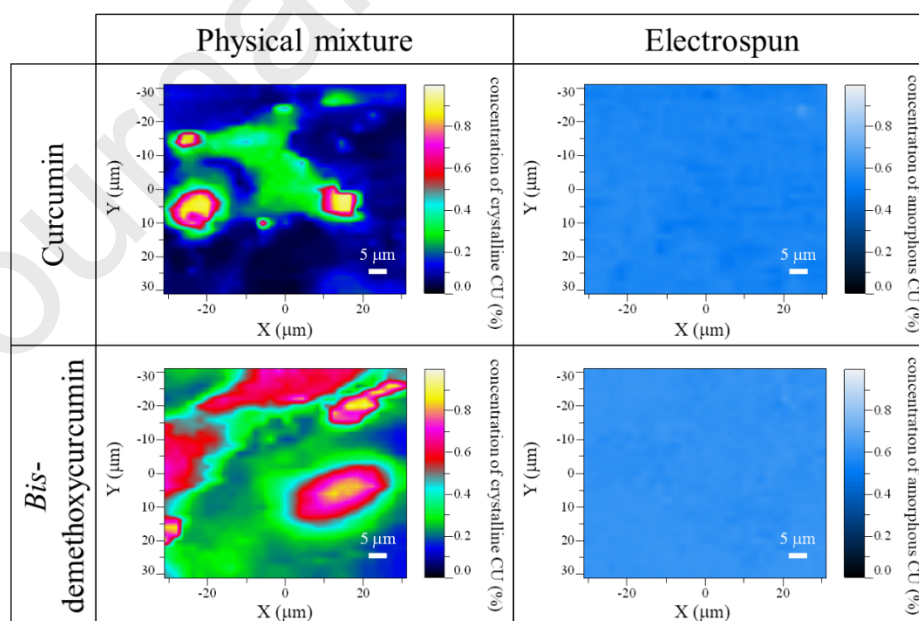


**Figure 10.** Raman maps of the physical mixture of CUR and CU4 and HP- $\beta$ -CD and the electrospun CU-HP- $\beta$ -CD complexes.

Raman map of both selected CUs physical mixtures (**Fig. 10**) shows uneven distribution, while the electrospun fibrous samples showed high uniformity. Consequently, the CU was uniformly distributed in the fibers (**Fig. 10**), which is essential for accurate dosing.

### 3.6. Dissolution test

The dissolution properties of the prepared complexes were evaluated by adding 1.5 mL of water (The small volume was selected because of the limited sample amounts.) to 800 mg electrospun (ES) samples. The vials were shaken vigorously after the water was added to them for 5 min, then the API concentration in the solution was measured with UV-VIS measurements (**Table 2**). The drug release was calculated by the API concentration in the solution after reconstitution and the API amount in the dissolved fibers. The drug release results were corrected with the water content of the samples. The resulting concentrations in the final reconstituted solutions are shown in **Table 2**.

**Table 2.** Comparison of solubility of the free APIs and the electrospun CU-HPBCD complexes and drug release results from the fibers (dissolution  $t=5$  min; solvent: ultrapure water pH=7).

Compound	Free API [CU] (mg/mL)	Electrospun CU-HP- $\beta$ -CD complex	Drug release from the solid fibers (%)
<b>CUR</b>	$1.1 \cdot 10^{-3}$	3.7	$99.7 \pm 2.1$
<b>CU2</b>	$3.8 \cdot 10^{-3}$	7.4	$99.2 \pm 1.8$
<b>CU3</b>	$4.2 \cdot 10^{-3}$	6.3	$100.0 \pm 1.0$
<b>CU4</b>	$4.7 \cdot 10^{-3}$	5.3	$99.5 \pm 2.0$

As seen in **Table 2**, the solubility of the fibrous CU-HP- $\beta$ -CD complexes was better by three orders of magnitude than the free APIs. The new formulation drastically improved the CUs solubility, and the presented formulation solution could be applied in general as the drug release was 100% in all cases.

Moreover, two selected electrospun (ES) CU and physical mixture (PM) samples were further compared to illustrate the improved dissolution properties. As it is visible on the recorded images (**Fig. 11**) the electrospun materials dissolved within 5 minutes, while the physical mixture did not dissolve in the same time frame.

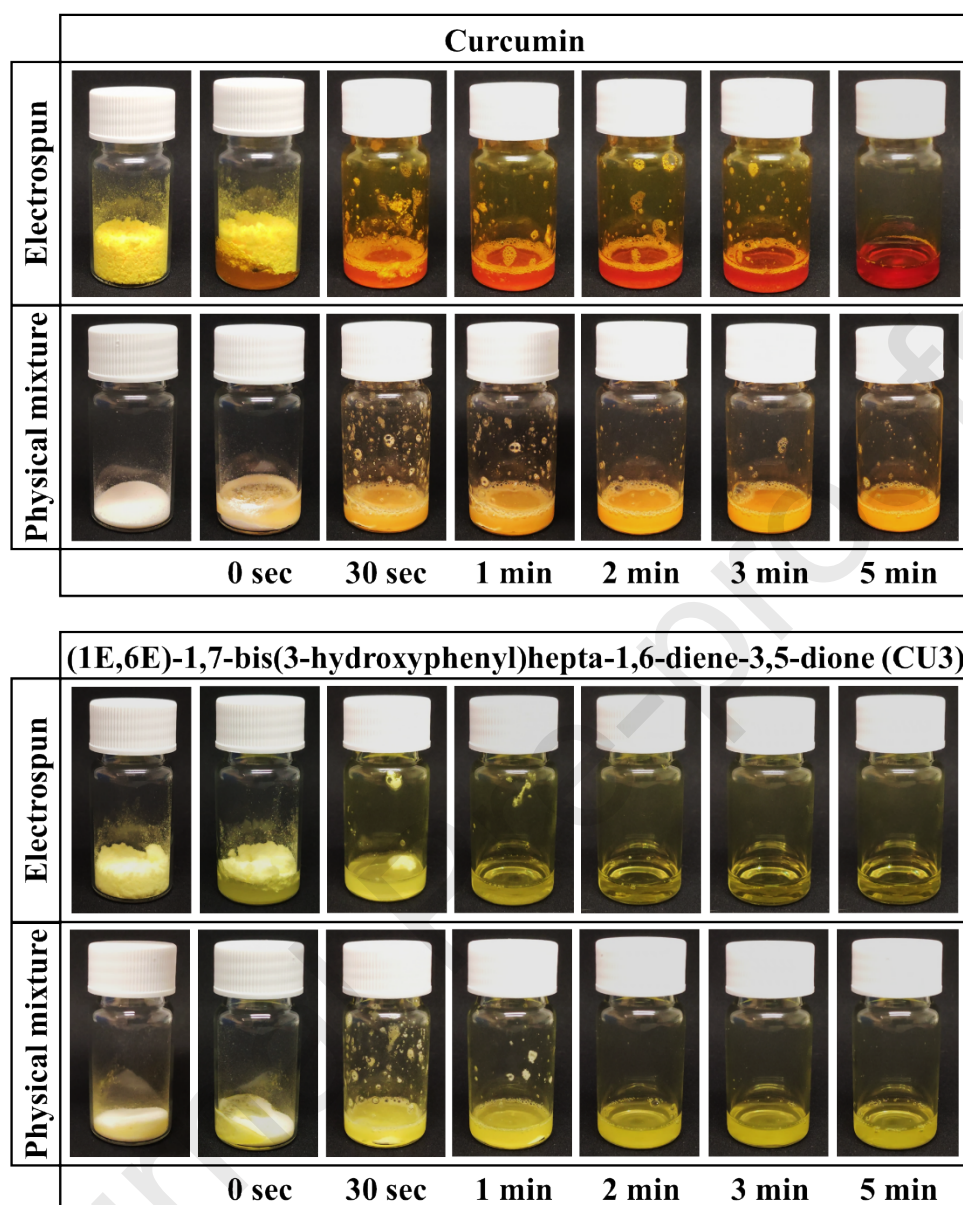
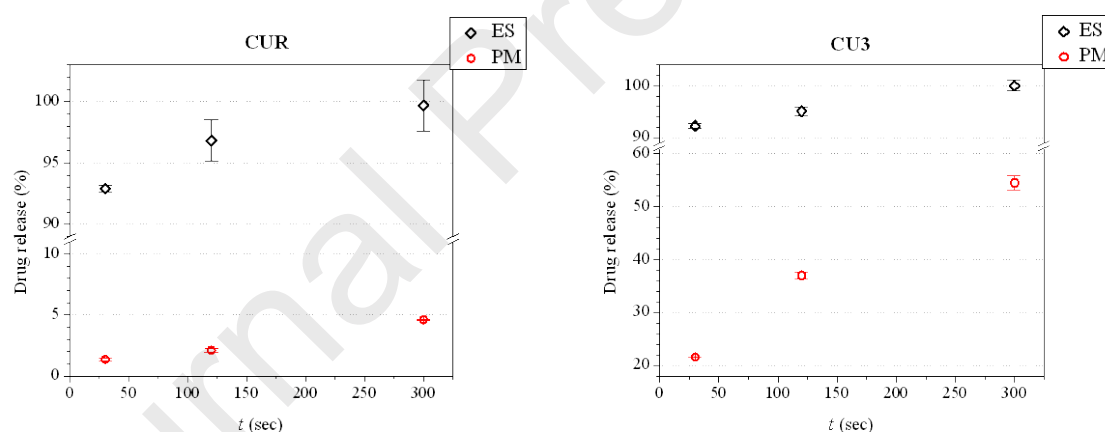


**Figure 11.** Images of the dissolution test of electrospun and the freeze-dried CU-HP- $\beta$ -CD complexes (CUR and CU3).

The difference between the dissolution rates of the electrospun sample and the physical mixture sample was confirmed by UV-VIS measurements after 30 s, 2 min, and 5 min of dissolution (**Fig. 12**). The results proved that the amorphous fibrous material provides fast and total dissolution, due to the added effects of the CU amorphous and complexed state and the enhanced specific surface area of the electrospun product. Compared to Celebioglu's work (Celebioglu and Uyar, 2020) we produced a fully dissolvable CUR-HP- $\beta$ -CD complex fiber and achieved higher CUR concentration in the final dissolution. Celebioglu tried to solve  $\sim 0.7$  mg CUR contained CUR-HP- $\beta$ -CD fiber in 5 mL water, which means the final CUR

concentration would be  $\sim 0.14$  mg/mL, however in their case the final solution was opaque, and they stated that there was still undissolved curcumin parts in solution. Where our CUR-HP- $\beta$ -CD fiber fully solved and the final CUR concentration in the solution was significantly higher with 3.7 mg/mL CUR.

Wang and colleagues (Wang et al., 2015) produced fast dissolving CUR loaded PVP K90 fibers ( $>90$  % CUR dissolution was observed within 15 min) – similarly to our work – for anticancer applications. However, our formulation had even faster dissolution (100% dissolution in 5 min), making the CUR-loaded HP- $\beta$ -CD fibers suitable to be used as a reconstitution product. Moreover, due to the applied PVP K90, Wang et al.'s final CUR formulation could not be used as an iv. product. PVP K90 is not advised to be used in parenteral products, due to the high molecular weight. Repeated dosing as a subcutaneous and intramuscular product shown subcutaneous granuloma (Robinson et al., 1990). The low molecular weight of HP- $\beta$ -CD, and the fast and total dissolution ensures that the electrospun final product discussed in this article has the potential to be used as a reconstitution iv. infusion product (if subsequent experiments confirm that the formulation is safe to use).



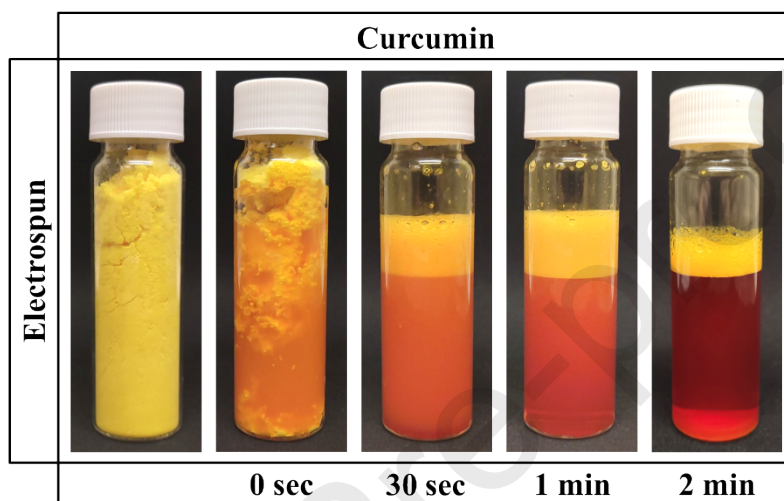
CUR	Electrospun (ES)	Physical mixture (PM)
30 s	(92.9 ± 0.3) %	(1.4 ± 0.1) %
2 min	(96.8 ± 1.7) %	(2.1 ± 0.2) %
5 min	(99.7 ± 2.1) %	(4.6 ± 0.1) %

CU3	Electrospun (ES)	Physical mixture (PM)
30 s	(92.3 ± 0.5) %	(21.6 ± 0.1) %
2 min	(95.1 ± 0.9) %	(37.0 ± 0.6) %
5 min	(100.0 ± 1.0) %	(54.4 ± 1.4) %

**Figure 12.** Dissolution test results of two selected CU-HP- $\beta$ -CD complexes (n=3). 100% equals the theoretical maximum concentration of the selected CUs.

In the case of infusion usage scenario, the water and electrospun materials amount can be multiplied compared to the case shown above. Infusion reconstitution is usually carried out in 20 mL water. To illustrate this, 6.0 g of CUR-HP- $\beta$ -CD were solved in 20 mL (Thus the CUR content was 42.0 mg). The recorded images (**Fig. 13**) shown fast dissolution time, as the sample was dissolved within 2 minutes (The total dissolution was verified with UV-VIS measurement;  $(99.6 \pm 1.2) \%$ ). With 6.0 g electrospun materials the API contents are in the range of 40-80 mg, which is similar to the currently proposed dose ( $<120 \text{ mg/m}^2$ ) (Storka et al., 2015).



**Figure 13.** Images of the large-scale dissolution test of electrospun CUR-HP- $\beta$ -CD complex.

The dissolution test results were corrected with the water content. The water content analyses of the electrospun CU-HP- $\beta$ -CD complexes and the physical mixtures were carried out with thermogravimetric analysis, the results shown in **Table S2**.

However, the HSES system used in the present work is not a fully closed, sterile manufacturing equipment and the presented formulation could not be used iv. without further investigations. This paper demonstrates only the opportunity for a new approach for using of curcuminoids in medicine as an anti-cancer product. To make a commercially available and safe iv. infusion product, the final reconstitution product must meet serious expectations which is discussed in the Pharmacopeias. One of the most critical tests in case of iv. products are defined in the USP <788> Particulate Matter in Injections (U.S. Pharmacopeia National Formulary, 2018), which describes requirements on the solution after reconstitution. The USP discusses two method options, in the more rigorous test the acceptable particle count does not exceed 3000 per container ( $\geq 10 \mu\text{m}$  particles) and 300 per container ( $\geq 25 \mu\text{m}$  particles) in small volume products ( $<100 \text{ mL}$ ).

Without the proper safety evaluation an iv. injection could cause embolism when it is injected directly into the circulatory system.

Therefore, the samples were checked in microscope to evaluate if there is any particle that is bigger than 10 or 25  $\mu\text{m}$ . Ten independent samples were measured twice, each sample contained 800 mg of fibrous CUR-HP- $\beta$ -CD in 1.5 mL ultrapure water (Particle size evaluation; **Supporting Info Section 3**). A sample picture could be seen in the **Supporting Info (Fig. S24)**. None of the samples contained bigger or equal particles in size than 10  $\mu\text{m}$  (average of 100 particle the size of them was  $2.22\pm 1.23$   $\mu\text{m}$ ), therefore, in the first approximation the electrospun final material meets the requirements which are given in the US Pharmacopeia.

### 3.7. *In vitro* cytostatic effect

To measure the antitumor activity of the electrospun CU-HP- $\beta$ -CD complexes in comparison with the free curcumin derivatives 4 different cell lines were selected. The  $\text{IC}_{50}$  values of the electrospun materials and the free APIs are presented in **Table 3**. The data indicate that the HP- $\beta$ -CD had no cytostatic effect on the cell lines in the applied concentration range. Overall, it can be concluded that CUs had slightly different activity on different cell lines. Nevertheless, the lowest cytostatic effect was shown on PANC-1 cell line that is usually the least sensitive to cytotoxic agents, while the highest activity was observed on the A2058 melanoma cell line on average. The electrospun samples were solved solely in water during the tests, while the CUs were solved with added DMSO to achieve adequate stock solution concentration. The free CUR (API) and the electrospun (ES) complexes were similar in activity, while the CU3 and CU4 complexes had slightly higher activity on the cell lines. In contrast, the CU2 complex had a drastically lower *in vitro* cytostatic effect – compared to the free API – on the selected cell lines, which could indicate, that the host-guest effect in this case was too high in the CU2-HP- $\beta$ -CD complex, therefore the HP- $\beta$ -CD might have inhibited the active site/group on the API.

**Table 3.** IC<sub>50</sub> values (μM) of the free APIs and the electrospun (ES) CU-HP-β-CD complexes.

Cell line	CUR		CU2		CU3		CU4		Free HP-β-CD
	Free API	ES	Free API	ES	Free API	ES	Free API	ES	
<b>A2058</b>	10.80 ± 0.73	12.18 ± 6.09	7.13 ± 0.46	>50	8.56 ± 0.47	5.91 ± 0.65	15.37 ± 1.04	11.49 ± 1.71	>100
<b>HT-29</b>	8.69 ± 4.62	18.67 ± 0.54	23.13 ± 2.16	>50	13.69 ± 1.25	8.42 ± 2.02	23.06 ± 9.08	19.32 ± 3.73	>100
<b>MDA-MB231</b>	16.02 ± 0.69	19.29 ± 1.40	21.39 ± 6.57	>50	11.89 ± 3.41	9.02 ± 1.17	22.36 ± 5.81	27.92 ± 1.16	>100
<b>PANC-1</b>	14.28 ± 0.69	19.00 ± 1.91	35.90 ± 0.94	>50	27.82 ± 9.30	15.12 ± 5.25	31.76 ± 1.88	>50	>100

The results indicate that if the selected CU and the HP-β-CD form a strong complex, the suggested formulation could not be used without significant activity loss. However, in the other cases, the formulation could be used without any significant loss of cytostatic effect, or even higher activity is achievable due to the higher solubility (and thus bioavailability) of the complex (while the free CUs were solved in DMSO, which itself could further induce the cytostatic effect). Moreover, the results suggest that the number and the orientation of the substituents on the aryl moiety could affect the cytostatic effect of the CUs. Their interaction with the HP-β-CD influences the accessibility of the CU. The **CU3** complex generally showed the highest cytostatic effect, surpassed even the **CUR** complex's effectiveness, while the **CU2** complex had the lowest cytostatic effect.

Compared the results to Chen and colleagues work (Chen et al., 2018), where they produced and studied the cytostatic effect of a CUR-β-CD polymer inclusion complex, were measured in 4 different cell lines (A375 - malignant melanoma, A549 - lung carcinoma, HeLa - Human cervix carcinoma and MCF-7 - breast cancer). None of the presented IC<sub>50</sub> were below 100 μM. Moreover, due to the used β-CD the product and the XRD measurement of the inclusion complex (which suggest that the CUR is not in amorphous state), the water solubility of this formulation could potentially be lower (β-CD water solubility at 25°C is <20g/L (Hedges, 2009); HP-β-CD, Kleptose® HPB (average degree of substitution = 0.62) is freely soluble in water (Roquette, 2021)).

Wang's (Wang et al., 2015) CUR containing PVP K90 fibers shown similar results to our work: the free CUR solved in DMSO had similar *in vitro* effects as the fibrous CUR. However, as

mentioned before, the PVP K90 is not advised to use in parenteral products (Robinson et al., 1990), therefore Wang's formulation could not be used as a potential iv. infusion product.

Journal Pre-proofs

## 4. Conclusions

In this work, a new solid CU-HP- $\beta$ -CD formulation was prepared with lab-scale and pilot-scale HSES. The applicability of the new formulation was shown with four different CUs. The electrospun CUs were amorphous and uniformly distributed in the fibers according to XRD analysis and Raman mappings. The fibers could be dissolved in water in a short time frame resulting in a particle-free solution. In typical iv. infusion reconstitution volume (20 mL) 40-80 mg of CU could be achieved, which is similar to the currently proposed dose (<120 mg/m<sup>2</sup>). The *in vitro* cytostatic effect data showed that the antitumor activity of the CU-HP- $\beta$ -CD complexes was similar to the free APIs or even better. Moreover, the electrospun samples were solved solely in water during the *in vitro* evaluation, while the free APIs were solved with added DMSO (adequate stock solution concentration is not achievable without DMSO) which could further increase the cytostatic effect. However, one complex ((1E,6E)-1,7-bis(3-hydroxyphenyl)hepta-1,6-diene-3,5-dione) had a significantly lower cytostatic effect, than the free API, thus indicating that aryl moiety-HP- $\beta$ -CD interaction could inhibit the cytostatic effect of the CUs. The results showed that there is a lot of potential in the presented CU-HP- $\beta$ -CD complex systems in cancer therapy. Moreover, the HSES technology combined with the HP- $\beta$ -CD complex system have the potential to bridge the gap in the CUs iv. application, due to it has high production rate and the applied HP- $\beta$ -CD is a safe, FDA approved excipient (even in iv. administration form). However, further experiments are needed to establish the CU-HP- $\beta$ -CD complexes safety as a reconstitution product for iv. infusion. Furthermore, the interactions between the CUs and the HP- $\beta$ -CD influences the anti-tumor effect of the API – which is worth investigating in further studies.

## Acknowledgements

The authors would like to thank László Simon for his help with the experiments.

## Funding

This work was supported by the National Research, Development and Innovation Office under grants NKFIH K119552, FK132133, ÚNKP-20-3-I and ÚNKP-21-4-II. Prepared with the professional support of the Doctoral Student Scholarship Program of the Co-operative Doctoral Program of the Ministry for Innovation and Technology from the source of the National Research, Development and Innovation Fund. A. Farkas acknowledges the financial support

received through the PREMIUM post-doctorate research program of the Hungarian Academy of Sciences later Eötvös Loránd Research Network. Support of grant BME FIKP-BIO by Ministry for Innovation and Technology is kindly acknowledged.

### **Conflicts of interest**

The authors declare no conflict of interest.

Journal Pre-proofs

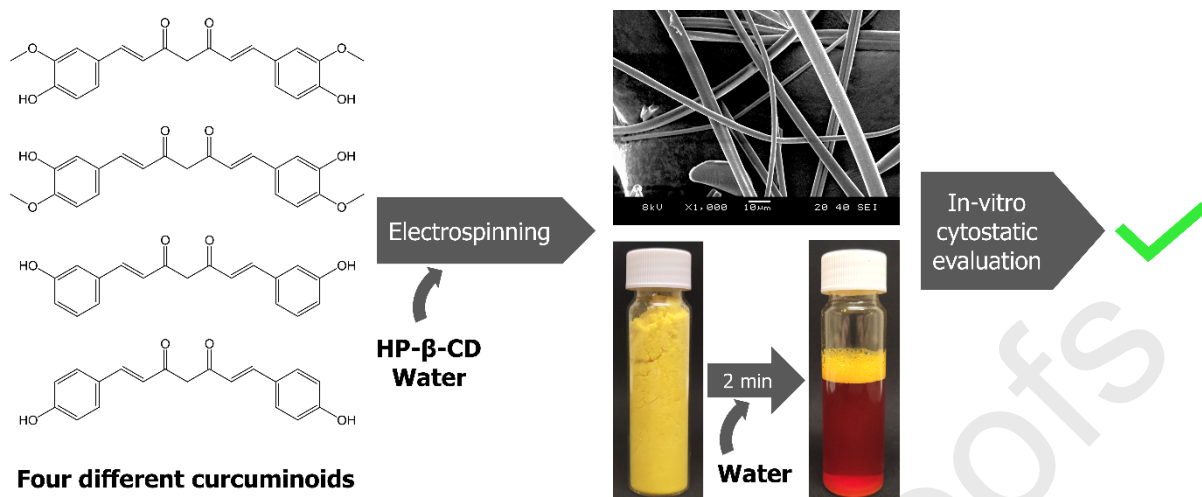
## References

- Al-Attar, T., Madihally, S. V., 2019. Targeted cancer treatment using a combination of siRNA-liposomes and resveratrol-electrospun fibers in co-cultures. *Int. J. Pharm.* 569, 118599. <https://doi.org/10.1016/j.ijpharm.2019.118599>
- Allafchian, A., Hosseini, H., Ghoreishi, S.M., 2020. Electrospinning of PVA-carboxymethyl cellulose nanofibers for flufenamic acid drug delivery. *Int. J. Biol. Macromol.* 163, 1780–1786. <https://doi.org/https://doi.org/10.1016/j.ijbiomac.2020.09.129>
- Amalraj, A., Pius, A., Gopi, Sreerag, Gopi, Sreeraj, 2017. Biological activities of curcuminoids, other biomolecules from turmeric and their derivatives – A review. *J. Tradit. Complement. Med.* 7, 205–233. <https://doi.org/10.1016/j.jtcme.2016.05.005>
- Awan, J.A., Rehman, S.U., Bangash, M.K., Ali, U., Asad, M., Hussain, F., Jaubert, J.-N., 2020. Development and characterization of electrospun curcumin-loaded antimicrobial nanofibrous membranes. *Text. Res. J.* 91, 1478–1485. <https://doi.org/10.1177/0040517520925514>
- Aytac, Z., Uyar, T., 2017. Core-shell nanofibers of curcumin/cyclodextrin inclusion complex and polylactic acid: Enhanced water solubility and slow release of curcumin. *Int. J. Pharm.* 518, 177–184. <https://doi.org/10.1016/j.ijpharm.2016.12.061>
- Bagad, A.S., Joseph, J.A., Bhaskaran, N., Agarwal, A., 2013. Comparative evaluation of anti-inflammatory activity of curcuminoids, turmerones, and aqueous extract of *Curcuma longa*. *Adv. Pharmacol. Sci.* 2013, 805756. <https://doi.org/10.1155/2013/805756>
- Bahrami, A., A. Ferns, G., 2020. Effect of curcumin and its derivatives on gastric cancer: molecular mechanisms. *Nutr. Cancer* 1–17. <https://doi.org/10.1080/01635581.2020.1808232>
- Balogh, A., Horváthová, T., Fülöp, Z., Loftsson, T., Harasztos, A.H., Marosi, G., Nagy, Z.K., 2015. Electroblowing and electrospinning of fibrous diclofenac sodium-cyclodextrin complex-based reconstitution injection. *J. Drug Deliv. Sci. Technol.* 26, 28–34. <https://doi.org/10.1016/j.jddst.2015.02.003>
- Brewster, M.E., Loftsson, T., 2007. Cyclodextrins as pharmaceutical solubilizers. *Adv. Drug Deliv. Rev.* 59, 645–666. <https://doi.org/10.1016/j.addr.2007.05.012>
- Bulboacă, A.E., Bolboacă, S.D., Stănescu, I.C., Sfrângeu, C.A., Porfire, A., Tefas, L., Bulboacă, A.C., 2018. The effect of intravenous administration of liposomal curcumin in addition to sumatriptan treatment in an experimental migraine model in rats. *Int. J. Nanomedicine* 13, 3093–3103. <https://doi.org/10.2147/IJN.S162087>
- Celebioglu, A., Uyar, T., 2021. Electrospun formulation of acyclovir/cyclodextrin nanofibers for fast-dissolving antiviral drug delivery. *Mater. Sci. Eng. C* 118, 111514. <https://doi.org/10.1016/j.msec.2020.111514>
- Celebioglu, A., Uyar, T., 2020. Fast-dissolving antioxidant curcumin/cyclodextrin inclusion complex electrospun nanofibrous webs. *Food Chem.* 317, 126397. <https://doi.org/10.1016/j.foodchem.2020.126397>
- Chen, J., Qin, X., Zhong, S., Chen, S., Su, W., Liu, Y., 2018. Characterization of curcumin/cyclodextrin polymer inclusion complex and investigation on its antioxidant and antiproliferative activities. *Molecules* 23, 1179. <https://doi.org/10.3390/molecules23051179>
- Chen, P., Wang, H., Yang, F., Chen, H., He, W., Wang, J., 2017. Curcumin promotes osteosarcoma cell death by activating miR-125a/ERR $\alpha$  signal pathway. *J. Cell. Biochem.* 118, 74–81. <https://doi.org/10.1002/jcb.25612>
- Chien, Y.W., 1991. Parenteral drug delivery and delivery systems, in: *Novel Drug Delivery Systems*.

- CRC Press, Boca Raton, USA, pp. 381–528. <https://doi.org/10.1201/b14196-9>
- Ding, Y., Dou, C., Chang, S., Xie, Z., Yu, D.-G., Liu, Y., Shao, J., 2020. Core–Shell Eudragit S100 Nanofibers Prepared via Triaxial Electrospinning to Provide a Colon-Targeted Extended Drug Release. *Polymers (Basel)*. 12. <https://doi.org/10.3390/polym12092034>
- FDA, 2017. FDA investigates two serious adverse events associated with ImprimisRx’s compounded curcumin emulsion product for injection [WWW Document]. URL <https://www.fda.gov/drugs/human-drug-compounding/fda-investigates-two-serious-adverse-events-associated-imprimisrxs-compounded-curcumin-emulsion> (accessed 9.15.21).
- Giordano, A., Tommonaro, G., 2019. Curcumin and cancer. *Nutrients* 11, 2376. <https://doi.org/10.3390/nu11102376>
- Gould, S., Scott, R.C., 2005. 2-Hydroxypropyl-beta-cyclodextrin (HP-beta-CD): a toxicology review. *Food Chem. Toxicol. an Int. J. Publ. Br. Ind. Biol. Res. Assoc.* 43, 1451–1459. <https://doi.org/10.1016/j.fct.2005.03.007>
- Greil, R., Greil-Ressler, S., Weiss, L., Schönlieb, C., Magnes, T., Radl, B., Bolger, G.T., Vcelar, B., Sordillo, P.P., 2018. A phase 1 dose-escalation study on the safety, tolerability and activity of liposomal curcumin (Lipocure™) in patients with locally advanced or metastatic cancer. *Cancer Chemother. Pharmacol.* 82, 695–706. <https://doi.org/10.1007/s00280-018-3654-0>
- Gupta, A.P., Khan, S., Manzoor, M.M., Yadav, A.K., Sharma, G., Anand, R., Gupta, S., 2017. Anticancer curcumin: natural analogues and structure-activity relationship, in: *Studies in Natural Products Chemistry*. Elsevier, Amsterdam, Netherlands, pp. 355–401. <https://doi.org/10.1016/B978-0-444-63929-5.00010-3>
- Hedges, A., 2009. Chapter 22 - Cyclodextrins: Properties and applications, in: BeMiller, J., Whistler, R.B.T.-S. (Third E. (Eds.), *Food Science and Technology*. Academic Press, San Diego, pp. 833–851. <https://doi.org/10.1016/B978-0-12-746275-2.00022-7>
- Jantarat, C., Sirathanarun, P., Ratanapongsai, S., Watcharakan, P., Sunyapong, S., Wadu, A., 2014. Curcumin-hydroxypropyl-β-cyclodextrin inclusion complex preparation methods: effect of common solvent evaporation, freeze drying, and pH shift on solubility and stability of curcumin. *Trop. J. Pharm. Res.* 13, 1215. <https://doi.org/10.4314/tjpr.v13i8.4>
- Kanu, N.J., Gupta, E., Vates, U.K., Singh, G.K., 2020. Electrospinning process parameters optimization for biofunctional curcumin/gelatin nanofibers. *Mater. Res. Express* 7, 35022. <https://doi.org/10.1088/2053-1591/ab7f60>
- Kurita, T., Makino, Y., 2013. Novel curcumin oral delivery systems. *Anticancer Res.* 33, 2807–2821.
- Kuttikrishnan, S., Siveen, K.S., Prabhu, K.S., Khan, A.Q., Ahmed, E.I., Akhtar, S., Ali, T.A., Merhi, M., Dermime, S., Steinhoff, M., Uddin, S., 2019. Curcumin induces apoptotic cell death via inhibition of PI3-kinase/AKT pathway in B-precursor acute lymphoblastic leukemia. *Front. Oncol.* 9, 484. <https://doi.org/10.3389/fonc.2019.00484>
- Lao, C.D., Ruffin, M.T., Normolle, D., Heath, D.D., Murray, S.I., Bailey, J.M., Boggs, M.E., Crowell, J., Rock, C.L., Brenner, D.E., 2006. Dose escalation of a curcuminoid formulation. *BMC Complement. Altern. Med.* 6, 10. <https://doi.org/10.1186/1472-6882-6-10>
- Li, D., Wang, M., Song, W.-L., Yu, D.-G., Bligh, S.W.A., 2021. Electrospun Janus Beads-On-A-String Structures for Different Types of Controlled Release Profiles of Double Drugs. *Biomolecules* 11. <https://doi.org/10.3390/biom11050635>
- Li, W., Zhou, Y., Yang, J., Li, H., Zhang, H., Zheng, P., 2017. Curcumin induces apoptotic cell death and protective autophagy in human gastric cancer cells. *Oncol. Rep.* 37, 3459–3466. <https://doi.org/10.3892/or.2017.5637>

- Loftsson, T., Jarho, P., Másson, M., Järvinen, T., 2005. Cyclodextrins in drug delivery. *Expert Opin. Drug Deliv.* 2, 335–351. <https://doi.org/10.1517/17425247.2.1.335>
- Mansouri, K., Rasoulpoor, Shna, Daneshkhan, A., Abolfathi, S., Salari, N., Mohammadi, M., Rasoulpoor, Shabnam, Shabani, S., 2020. Clinical effects of curcumin in enhancing cancer therapy: A systematic review. *BMC Cancer* 20, 791. <https://doi.org/10.1186/s12885-020-07256-8>
- Menon, V.P., Sudheer, A.R., 2007. Antioxidant and anti-inflammatory properties of curcumin. *Adv. Exp. Med. Biol.* 595, 105–125. [https://doi.org/10.1007/978-0-387-46401-5\\_3](https://doi.org/10.1007/978-0-387-46401-5_3)
- Nagy, Z.K., Balogh, A., Démuth, B., Pataki, H., Vigh, T., Szabó, B., Molnár, K., Schmidt, B.T., Horák, P., Marosi, G., Verreck, G., Van Assche, I., Brewster, M.E., 2015. High speed electrospinning for scaled-up production of amorphous solid dispersion of itraconazole. *Int. J. Pharm.* 480, 137–142. <https://doi.org/10.1016/j.ijpharm.2015.01.025>
- Nagy, Z.K., Balogh, A., Vajna, B., Farkas, A., Patyi, G., Kramarics, Á., Marosi, G., 2012. Comparison of electrospun and extruded soluplus®-based solid dosage forms of improved dissolution. *J. Pharm. Sci.* 101, 322–332. <https://doi.org/10.1002/jps.22731>
- Ouyang, H.-Z., Fang, L., Zhu, L., Zhang, L., Ren, X.-L., He, J., Qi, A.-D., 2012. Effect of external factors on the curcumin/2-hydroxypropyl- $\beta$ -cyclodextrin: in vitro and in vivo study. *J. Incl. Phenom. Macrocycl. Chem.* 73, 423–433. <https://doi.org/10.1007/s10847-011-0080-x>
- Ramalingam, N., Natarajan, T.S., Rajiv, S., 2015. Preparation and characterization of electrospun curcumin loaded poly(2-hydroxyethyl methacrylate) nanofiber--a biomaterial for multidrug resistant organisms. *J. Biomed. Mater. Res. A* 103, 16–24. <https://doi.org/10.1002/jbm.a.35138>
- Razzaq, A., Khan, Z.U., Saeed, A., Shah, K.A., Khan, N.U., Menaa, B., Iqbal, H., Menaa, F., 2021. Development of cephradine-loaded gelatin/polyvinyl alcohol electrospun nanofibers for effective diabetic wound healing: in-vitro and in-vivo assessments. *Pharmaceutics* 13. <https://doi.org/10.3390/pharmaceutics13030349>
- Reddy, A.R., Dinesh, P., Prabhakar, A.S., Umasankar, K., Raju, B.S. and M.B., 2013. A comprehensive review on SAR of curcumin. *Mini-Reviews Med. Chem.* 13, 1769–1777. <https://doi.org/10.2174/1389557511313120007>
- Robinson, B.V., Sullivan, F.M., Borzelleca, J.F., Schwartz, S.L., 1990. PVP: A critical review of the kinetics and toxicology of polyvinylpyrrolidone (Povidone), 1st ed. CRC Press, Boca Raton, USA. <https://doi.org/10.1201/9780203741672>
- Roquette, 2021. Quality specification sheet - Kleptose® HPB parenteral grade [WWW Document]. URL [https://www.roquette.com/-/media/roquette-sharepoint-libraries/product-specification-sheet/2021/09/30/23/07/roquette\\_quality\\_specification-sheet\\_kleptose-hpb-parenteral-grade\\_50\\_346111\\_en.pdf](https://www.roquette.com/-/media/roquette-sharepoint-libraries/product-specification-sheet/2021/09/30/23/07/roquette_quality_specification-sheet_kleptose-hpb-parenteral-grade_50_346111_en.pdf) (accessed 9.21.21).
- Sasmal, P., Datta, P., 2019. Tranexamic acid-loaded chitosan electrospun nanofibers as drug delivery system for hemorrhage control applications. *J. Drug Deliv. Sci. Technol.* 52, 559–567. <https://doi.org/10.1016/j.jddst.2019.05.018>
- Sebe, I., Szabó, B., Nagy, Z.K., Szabó, D., Zsidai, L., Kocsis, B., Zelkó, R., 2013. Polymer structure and antimicrobial activity of polyvinylpyrrolidone-based iodine nanofibers prepared with high-speed rotary spinning technique. *Int. J. Pharm.* 458, 99–103. <https://doi.org/10.1016/j.ijpharm.2013.10.011>
- Shababdoust, A., Ehsani, M., Shokrollahi, P., Zandi, M., 2018. Fabrication of curcumin-loaded electrospun nanofibrous polyurethanes with anti-bacterial activity. *Prog. Biomater.* 7, 23–33. <https://doi.org/10.1007/s40204-017-0079-5>
- Sharma, R.A., Euden, S.A., Platton, S.L., Cooke, D.N., Shafayat, A., Hewitt, H.R., Marczylo, T.H.,

- Morgan, B., Hemingway, D., Plummer, S.M., Pirmohamed, M., Gescher, A.J., Steward, W.P., 2004. Phase I clinical trial of oral curcumin: biomarkers of systemic activity and compliance. *Clin. cancer Res. an Off. J. Am. Assoc. Cancer Res.* 10, 6847–6854. <https://doi.org/10.1158/1078-0432.CCR-04-0744>
- Shehzad, A., Lee, J., Lee, Y.S., 2013. Curcumin in various cancers. *BioFactors* 29, 56–68. <https://doi.org/10.1002/biof.1068>
- Sökmen, M., Akram Khan, M., 2016. The antioxidant activity of some curcuminoids and chalcones. *Inflammopharmacology* 24, 81–86. <https://doi.org/10.1007/s10787-016-0264-5>
- Storka, A., Vcelar, B., Klickovic, U., Gouya, G., Weisshaar, S., Aschauer, S., Bolger, G., Helson, L., Wolzt, M., 2015. Safety, tolerability and pharmacokinetics of liposomal curcumin in healthy humans. *Int. J. Clin. Pharmacol. Ther.* 53, 54–65. <https://doi.org/10.5414/CP202076>
- Sun, X.-Z., Williams, G.R., Hou, X.-X., Zhu, L.-M., 2013. Electrospun curcumin-loaded fibers with potential biomedical applications. *Carbohydr. Polym.* 94, 147–153. <https://doi.org/10.1016/j.carbpol.2012.12.064>
- Tipduangta, P., Belton, P., McAuley, W.J., Qi, S., 2021. The use of polymer blends to improve stability and performance of electrospun solid dispersions: The role of miscibility and phase separation. *Int. J. Pharm.* 602, 120637. <https://doi.org/10.1016/j.ijpharm.2021.120637>
- Tomeh, M.A., Hadianamrei, R., Zhao, X., 2019. A review of curcumin and its derivatives as anticancer agents. *Int. J. Mol. Sci.* 20, 1033. <https://doi.org/10.3390/ijms20051033>
- Topuz, F., Uyar, T., 2019. Electrospinning of cyclodextrin functional nanofibers for drug delivery applications. *Pharmaceutics* 11, 6. <https://doi.org/10.3390/pharmaceutics11010006>
- Tuğcu-Demiröz, F., Saar, S., Tort, S., Acartürk, F., 2020. Electrospun metronidazole-loaded nanofibers for vaginal drug delivery. *Drug Dev. Ind. Pharm.* 46, 1015–1025. <https://doi.org/10.1080/03639045.2020.1767125>
- U.S. Pharmacopeia National Formulary, 2018. Particulate Matter in Injections, in: U.S. Pharmacopeia National Formulary. The United States Pharmacopeial Convention, Rockville, MD, pp. 6537–6540.
- Wagner, A., Vorauer-Uhl, K., 2011. Liposome technology for industrial purposes. *J. Drug Deliv.* 2011, 591325. <https://doi.org/10.1155/2011/591325>
- Wang, C., Ma, C., Wu, Z., Liang, H., Yan, P., Song, J., Ma, N., Zhao, Q., 2015. Enhanced bioavailability and anticancer effect of curcumin-loaded electrospun nanofiber: In vitro and in vivo study. *Nanoscale Res. Lett.* 10, 439. <https://doi.org/10.1186/s11671-015-1146-2>
- Wang, Y., Yu, J., Cui, R., Lin, J., Ding, X., 2016. Curcumin in treating breast cancer: a review. *J. Lab. Autom.* 21, 723–731. <https://doi.org/10.1177/2211068216655524>
- Yang, K.-Y., Lin, L.-C., Tseng, T.-Y., Wang, S.-C., Tsai, T.-H., 2007. Oral bioavailability of curcumin in rat and the herbal analysis from *Curcuma longa* by LC-MS/MS. *J. Chromatogr. B. Analyt. Technol. Biomed. Life Sci.* 853, 183–189. <https://doi.org/10.1016/j.jchromb.2007.03.010>
- Zare, M.R., Khorram, M., Barzegar, S., Asadian, F., Zarehshahabadi, Z., Saharkhiz, M.J., Ahadian, S., Zomorodian, K., 2021. Antimicrobial core-shell electrospun nanofibers containing Ajwain essential oil for accelerating infected wound healing. *Int. J. Pharm.* 603, 120698. <https://doi.org/10.1016/j.ijpharm.2021.120698>
- Zheng, X., Kang, S., Wang, K., Yang, Y., Yu, D.-G., Wan, F., Williams, G.R., Bligh, S.-W.A., 2021. Combination of structure-performance and shape-performance relationships for better biphasic release in electrospun Janus fibers. *Int. J. Pharm.* 596, 120203. <https://doi.org/10.1016/j.ijpharm.2021.120203>



**Krisztina Kiss:** Conceptualization, Formal analysis, Investigation, Writing - Original Draft, Visualization, Funding acquisition. **Kristóf Hegedüs:** Conceptualization, Investigation, Writing - Original Draft. **Panna Vass:** Conceptualization, Investigation, Writing - Review & Editing, Funding acquisition. **Diána Vári-Mező:** Formal analysis, Investigation, Writing - Original Draft. **Attila Farkas:** Formal analysis, Investigation, Funding acquisition. **Zsombor Kristóf Nagy:** Writing - Review & Editing, Funding acquisition. **László Molnár:** Writing - Review & Editing. **József Tóvári:** Writing - Review & Editing, Funding acquisition. **Gábor Mező:** Writing - Review & Editing, Funding acquisition. **György Marosi:** Writing - Review & Editing, Supervision, Funding acquisition.

#### Declaration of interests

- The authors declare that they have no known competing financial interests or personal relationships that could have appeared to influence the work reported in this paper.
- The authors declare the following financial interests/personal relationships which may be considered as potential competing interests: